Original Article

JCBFM

Journal of Cerebral Blood Flow & Metabolism
2021, Vol. 41(10) 2725–2742

DOI: 10.1177/0271678X211010351
journals.sagepub.com/home/jcbfm
SAGE

Genetic deletion of endothelial microRNA-15a/16-1 promotes cerebral angiogenesis and neurological recovery in ischemic stroke through Src signaling pathway

Ping Sun[1], Feifei Ma[1], Yang Xu[1], Chao Zhou[1], R. Anne Stetler[1] and Ke-Jie Yin[1,2]

Abstract

Cerebral angiogenesis is tightly controlled by specific microRNAs (miRs), including the miR-15a/16-1 cluster. Recently, we reported that endothelium-specific conditional knockout of the miR-15a/16-1 cluster (EC-miR-15a/16-1 cKO) promotes post-stroke angiogenesis and improves long-term neurological recovery by increasing protein levels of VEGFA, FGF2, and their respective receptors VEGFR2 and FGFR1. Herein, we further investigated the underlying signaling mechanism of these pro-angiogenic factors after ischemic stroke using a selective Src family inhibitor AZD0530. EC-miR-15a/16-1 cKO and age- and sex-matched wild-type littermate (WT) mice were subjected to 1 h middle cerebral artery occlusion (MCAO) and 28d reperfusion. AZD0530 was administered daily by oral gavage to both genotypes of mice 3-21d after MCAO. Compared to WT, AZD0530 administration exacerbated spatial cognitive impairments and brain atrophy in EC-miR-15a/16-1 cKO mice following MCAO. AZD0530 also attenuated long-term recovery of blood flow and inhibited the formation of new microvessels, including functional vessels with blood circulation, in the penumbra of stroked cKO mice. Moreover, AZD0530 blocked the Src signaling pathway by downregulating phospho-Src and its downstream mediators (p-Stat3, p-Akt, p-FAK, p-p44/42 MAPK, p-p38 MAPK) in post-ischemic brains. Collectively, our data demonstrated that endothelium-targeted deletion of the miR-15a/16-1 cluster promotes post-stroke angiogenesis and improves long-term neurological recovery via activating Src signaling pathway.

Keywords

Brain vascular endothelial cells, miR-15a/16-1, ischemic stroke, angiogenesis, Src signaling pathway

Received 2 November 2020; Revised 13 March 2021; Accepted 18 March 2021

Introduction

Stroke remains the second leading cause of death and the leading cause of long-term disability in adults worldwide.[1] As the most common stroke type, cerebral ischemia is characterized by severe focal cerebral blood flow reduction, which ultimately leads to neuronal death and infarction in affected brain tissues. Current therapeutics, including tPA-mediated thrombolysis and endovascular thrombectomy, can only be applied to eligible patients who meet the clinical criteria within a limited time window.[2] A large number of patients still undergo severe brain impairment after the onset of ischemic stroke, thus necessitating a focus on

[1]Pittsburgh Institute of Brain Disorders and Recovery, Department of Neurology, University of Pittsburgh School of Medicine, Pittsburgh, PA, USA
[2]Geriatric Research, Education and Clinical Center, Veterans Affairs Pittsburgh Healthcare System, Pittsburgh, PA, USA

Corresponding authors:
Ke-Jie Yin, Pittsburgh Institute of Brain Disorders & Recovery and Department of Neurology, University of Pittsburgh School of Medicine, 200 Lothrop Street, BST S514, Pittsburgh, PA 15213, USA.
Email: yink2@upmc.edu

R. Anne Stetler, Pittsburgh Institute of Brain Disorders & Recovery and Department of Neurology, University of Pittsburgh School of Medicine, 3500 Terrace Street, BST S521, Pittsburgh, PA 15213, USA.
Email: stetler@pitt.edu

functional recovery as a central component for post-stroke rehabilitation.[3] In this context, accumulating evidence indicates that cerebral angiogenesis occurs in patients following ischemic stroke, which is associated with improved survival.[4,5] Stroke can rapidly trigger the induction and activation of various vital angiogenic factors involved in the development of angiogenesis, including vascular endothelial growth factor (VEGF),[6,7] basic fibroblast growth factor (bFGF),[8,9] platelet-derived growth factor (PDGF),[10,11] transforming growth factor-beta (TGF-β),[12,13] angiopoietins,[14,15] and neuropilin-1.[16] Moreover, restoration of cerebral microvasculature after stroke can stimulate other endogenous recovery mechanisms involving neurogenesis, synaptogenesis, and neuronal and synaptic plasticity.[17] Thus, promoting cerebral angiogenesis has become an attractive therapeutic strategy for effective improvement of stroke recovery.

MicroRNAs (miRs) represent a novel class of endogenous single-stranded small non-coding RNA molecules (~21–25 nucleotide) that post-transcriptionally suppress gene expression by hybridizing to 3′-untranslated regions (3'-UTR) of target mRNAs in a sequence-specific manner.[18] MiRs play critical regulatory roles in various cellular processes under both physiological and pathological conditions. Recent studies underscore the importance and therapeutic potentials of miRs in the central nervous system (CNS) injuries, including ischemic stroke, as well as in the regulation of vascular endothelial function or angiogenesis with or without stroke conditions.[19–21] Among these miRs, miR-15a and miR-16-1 are two closely located and highly conserved miRs. miR-15a and miR-16-1 form as a structural and functional cluster (the miR-15a/16-1 cluster) by simultaneously binding to their common mRNA targets.[22,23] miR-15a and miR-16-1 expression are markedly upregulated in ischemic brain in stroke animals models[23,24] and are elevated in serum of stroke patients with positive correlation to clinical outcomes, thus suggesting they may serve as potential non-invasive biomarkers for acute ischemic stroke.[25–27]

miR-15a and miR-16-1 are also promising targets for regulating angiogenesis toward tissue repair. We previously discovered that vascular endothelial cell-selective overexpression of miR-15a/16-1 (EC-miR-15a/16-1 TG) suppresses hindlimb ischemia-induced cell-autonomous angiogenesis in peripheral circulating blood vessels.[28] Moreover, by using an endothelial cell-selective miR-15a/16-1 conditional knockout (EC-miR-15a/16-1 cKO) mouse model, we further investigated the long-term impact and its underlying molecular mechanisms of endothelial miR-15a/16-1 on post-ischemia angiogenesis.[24] We demonstrated that endothelium-targeted deletion of the miR-15a/16-1 cluster robustly promotes post-stroke brain angiogenesis, improves long-term neurological recovery, and upregulates the protein expression of proangiogenic factors vascular endothelial growth factor (VEGFA), fibroblast growth factor 2 (FGF2), and their respective receptors vascular endothelial growth factor receptor 2 (VEGFR2) and fibroblast growth factor receptor 1 (FGFR1) after ischemic stroke.[24] However, the downstream molecular mechanism that underlies miR-15a/16-1-afforded effect on post-stroke angiogenesis remains elusive.

Src kinase regulates the proliferation and differentiation of vascular endothelial cells, and can regulate angiogenesis induced by a wide range of stimuli, including angiogenic factors VEGFA[29,30] and FGF2.[31,32] Eliceiri et al. demonstrated that Src kinase activity is required for VEGF-induced angiogenesis in chick embryos and in a mouse model of subcutaneous angiogenesis.[30] Similarly, Klint et al. showed that Src kinase activity might be a prerequisite for FGF2-induced capillary endothelial cell differentiation, as treatment with a Src kinase inhibitor PP1 abrogated tube formation in murine brain capillary endothelial cells.[32] Sandilands et al. also found that Src kinase activity plays a crucial role in mediating and modulating the activation, transport, and signaling dynamics of FGF2-activated fibroblast growth factor receptors in mouse embryo fibroblasts (MEFs).[31]

Src kinase is also involved in growth factor-induced vascular permeability, blood-brain barrier breakdown, and cerebral angiogenesis after ischemic stroke. Paul et al. reported that genetic deletion of Src or pharmacological inhibition of Src activity protects against VEGF-mediated vascular permeability at 24 h after focal cerebral ischemia in mice.[33] However, pharmacological blockade of Src activity during chronic stages of post-stroke brain recovery impaired n-3 PUFA-enhanced angiogenesis and exacerbated long-term neurological deficits.[34] Therefore, the present study was to test the hypothesis that Src kinase is an important modulator for endothelial miR-15a/16-1 in the regulation of post-stroke angiogenesis and neurological recovery. Indeed, our results demonstrate that the Src signaling is a critical downstream component of VEGFA and FGF2 signaling and contributes to the proangiogenic effects afforded by EC-selective conditional knockout of miR-15a/16-1 after ischemic stroke.

Material and methods

Animals

All procedures were approved by the University of Pittsburgh Institutional Animal Care and Use Committee and performed in accordance with the

National Institutes of Health Guide for the Care and Use of Laboratory Animals. All experiments were reported in compliance with the ARRIVE guidelines 2.0 (ARRIVE, Animal Research: Reporting in Vivo Experiments).[35] Endothelium-targeted miR-15a/16-1 conditional knockout (EC-miR-15a/16-1 cKO) mice[24] were generated on C57BL6/J background, by cross-mating miR-15a/16-1$^{flox/flox}$ mice (a generous gift from Dr. Riccardo Dallla-Favera at Columbia University)[36] with VE-Cadherin Cre transgenic mice.[37] EC-miR-15a/16-1 cKO mice were viable and fertile with normal appearance, behavior, growth, and litter size. All mice were housed in a room where the lighting was controlled (12 h on, and 12 h off) and the room temperature was kept around 22°C. Mice were given a standard diet and water *ad libitum*. All efforts were made to minimize animal suffering and the number of experimental animals.

Mouse model of transient focal cerebral ischemia

Focal cerebral ischemia was induced by transient middle cerebral artery occlusion (tMCAO).[23,24,38,39] Briefly, male mice (8–10 weeks, 23–26 g) were anesthetized with isoflurane (3% for induction, 1.5% for maintenance) in mixed O_2 and N_2O (30%:67%). After a midline skin incision, the common carotid artery was exposed, and then its branches were electro-coagulated. A 1.3-cm length of a 7-0 rounded tip nylon suture (Doccol Corporation, Sharon, MA) was gently advanced from the external carotid artery to the internal carotid artery and further to the origin of the middle cerebral artery (MCA) until regional CBF was reduced to ~25% of baseline. After 60 minutes of MCA occlusion, blood flow was restored by removing the suture. After reperfusion from MCAO, the mice were allowed to recover, and body temperature was measured with a rectal thermometer was maintained at 37.0 ± 0.5°C by a temperature-controlled heating pad during the ischemic period. Regional CBF was measured using a laser speckle imager (Perimed PeriCam PSI HR, Stockholm, Sweden) at 15 min before MCAO surgery, 15 min during MCAO period, and 15 min after the onset of reperfusion. The analgesic ketoprofen (3 mg/kg) was injected intramuscularly to the animal immediately prior to MCAO surgery and twice a day for the following 2 days post-surgery. Animals that fulfilled the exclusion criteria (see Supplemental Methods) during/after MCAO were excluded from the data analyses (Figure S2).

Laser speckle imaging

Laser speckle imaging (Perimed PeriCam PSI HR, Stockholm, Sweden) was used to monitor the regional CBF after MCAO as described previously.[34,40] Briefly, mice were anesthetized (3% for induction, 1.5% for maintenance) and the head was fixed in a head holder in a prone position. The scalp was shaved, and a middle incision was made to expose the skull. The skull surface was illuminated by a laser diode (785 nm), which allowed the laser to penetrate through the brain in a diffused manner. CBF was measured by speckle contrast, which is the ratio of the standard deviation of pixel intensity to mean pixel intensity, representing the speckle visibility relative to the velocity of the light-scattering particles (blood). The speckle contrast was then converted to correlation time values, which are inversely proportional to mean blood flow velocity. Two-dimensional microcirculation images were captured 15 min before MCAO, 15 min after the onset of MCAO, and 15 min, 3 d, 7 d, 14 d, 21 d, and 28 d after the onset of reperfusion. For each animal, five consecutive images were captured at each time point. For image data analysis, two identical elliptical regions of interest (ROIs) were created on ipsilateral and the contralateral hemispheres of each image. The blood flow perfusion index was first determined as the ratio of ischemic to non-ischemic CBF and then further normalized to the presurgical baseline to obtain the relative CBF value for each animal.

CD31 immunofluorescence staining

CD31 immunofluorescence staining was used to detect the brain microvasculature as previously described.[24] Briefly, after a series of washes with 0.3% PBST (0.3% Triton X-100 in PBS), free-floating brain sections were incubated with 1% PBST for 20 min, followed by blocking with 5% normal donkey serum for 1 h. After a series of washes with 0.3% PBST, brain sections were incubated overnight at 4°C with rat anti-mouse CD31 (1:200, BD Pharmingen). After another series of washes, brain sections were then incubated with Alexa Fluor 488 conjugated donkey anti-rat secondary antibody (1:400, Jackson ImmunoResearch Laboratories). For CD31 and phosphorylated-Src (P-Src) double-immunostaining, brain sections were further washed with 0.3% PBST, and blocked with 5% normal donkey serum for 1 h. After a series of washes with 0.3% PBST, brain sections were incubated overnight at 4°C with rabbit anti-mouse P-Src (1:200, Cell Signaling). After another series of washes, sections were incubated with Cy3 AffiniPure Donkey Anti-Rabbit IgG (1:400, Jackson ImmunoResearch Laboratories) for 1 h at RT in the dark. The sections were mounted with VECTASHIELD Hard Set mounting medium. The immunofluorescence images were captured with an Olympus Fluoview FV1000 confocal microscope with FV10-ASW 2.0 software (Olympus

America, Center Valley, PA). Regions of interest (Figure S3) from the ischemic boundary zone (IBZ) were selected and scanned at 1024×1024 pixels ($626.6 \times 626.6\,\mu m^2$) format in the x-y direction, and 1-μM step-size optical sections along the z-axis were acquired with a $20\times$ objective lens. Three-dimensional (3D) reconstruction was performed by Adobe Photoshop CC 2018 software or the imaging processing software Imaris (Bitplane, Belfast, United Kingdom) as described previously.[42] The vascular density, the vascular surface area (mm^2), vascular length (mm), branch points and capillary number per volume of tissue (mm^3) were quantified with the NIH ImageJ software in a blinded manner.

Functional vessel labeling

Tomato lectin can selectively bind to endothelial glycocalyx in perfused vessels, thus it was used to label functional vessels in the brain as described previously.[24,34] Briefly, mice were anesthetized and transcardially perfused with biotin-conjugated tomato lectin (10 mg/kg, Vector Labs, Burlingame, USA) 5 min before euthanasia. Then, the mice were perfused with 0.9% NaCl followed by 4% paraformaldehyde in PBS. Coronal brain sections were prepared as described above. After a series of washes with 0.3% PBST (0.3% Triton X-100 in PBS), free-floating sections were incubated with 1% PBST for 20 min, followed by blocking with 5% normal donkey serum for 1 h. After another series of washes with 0.3% PBST, brain sections were incubated with Alexa Fluor® 488 streptavidin (1: 1000, Jackson ImmunoResearch Laboratories) at room temperature (RT) in the dark for 1 h. Images were captured and analyzed with the same methods as CD31 immunostaining described above.

BrdU labeling of newly proliferated cells

Newly proliferated cells were labeled with the S-phase marker 5-bromo-2'-deoxyuridine (BrdU, Sigma Aldrich) as described.[24] Briefly, BrdU (50 mg/kg body weight) was injected intraperitoneally (i.p.) twice per day with an interval of 6 h at 3–6 d after MCAO (Figure S1). Coronal brain sections were prepared as described above. After a series of washes with PBS, brain sections were pretreated in 1 N HCl for 1 h followed by 0.1 M boric acid (pH 8.5) for 10 min at RT. Sections were then blocked with 5% normal donkey serum in 0.3% PBST for 1 h, followed by blocking with M.O.M kit (Vector Laboratories) for 1 h at RT, incubating with purified mouse anti-BrdU antibody (1:200, BD Pharmingen) for 1 h at RT, and then continuing to incubate overnight at 4°C. After a series of washes, sections were incubated with Cy3 AffiniPure Donkey Anti-Mouse IgG (1:400, Jackson ImmunoResearch Laboratories) for 1 h at RT in the dark. The sections were mounted with VECTASHIELD Hard Set mounting medium, and images were captured with an Olympus Fluoview FV1000 confocal microscope with FV10-ASW 2.0 software. Regions of interest (Figure S3) were selected and scanned in the peri-infarct areas of each section, as described above. BrdU immunopositive cells were counted using ImageJ and calculated as the number of $BrdU^+$ cells in the designated fields divided by the volume (mm^3). Newly formed microvessels were assessed by counting BrdU immunopositive cells along the microvessels in BrdU/CD31 double-immunostained sections. Newly formed functional vessels were assessed by counting BrdU immunopositive signals among blood vessels in BrdU/Tomato-lectin double-immunostained sections.

Results

Src kinase is activated in the peri-infarct brain regions of EC-targeted miR-15a/16-1 cKO mice after focal cerebral ischemia

Src kinase can mediate the angiogenic signaling transduction in response to a variety of growth factors, including VEGFA[29,30] and FGF2.[31,32] Thus, in order to explore if Src signaling cascades are involved in EC-miR-15a/16-1 regulated angiogenesis and function recovery, we first determined the co-localization of cerebral microvessels (CD31) and phosphorylated Src kinase (P-Src) in the peri-infarct regions of ischemic brains in EC-miR-15a/16-1 WT and cKO mice at 14 days after tMCAO. As shown in Figure 1(a) to (d), representative images (a–c) and quantitative analysis (d) demonstrated that higher levels of P-Src signals were present in the cerebral microvessels in the peri-infarcted areas of miR-15a/16-1 cKO mouse brains, compared to WT controls. There were almost no positive P-Src signals in the sham controls. We further examined the protein expression of total and phosphorylated Src kinase in the ischemic cortical regions of WT and EC-miR-15a/16-1 cKO mice at 14 days after tMCAO by western blotting (WB, specific antibodies are detailed in **Table S2**). Representative WB images (Figures 1(e) and S9) and quantitative analysis (Figure 1(f) and (g)) showed that endothelium-targeted deletion of miR-15a/16-1 cluster significantly elevated phosphorylated Src protein ($^{***}p = 6.31 \times 10^{-5}$), but not the total Src protein, in the post-ischemic cortex compared to WT mice. Treatment of AZD0530, a selective Src kinase inhibitor, significantly attenuated the enhanced cortical protein levels of

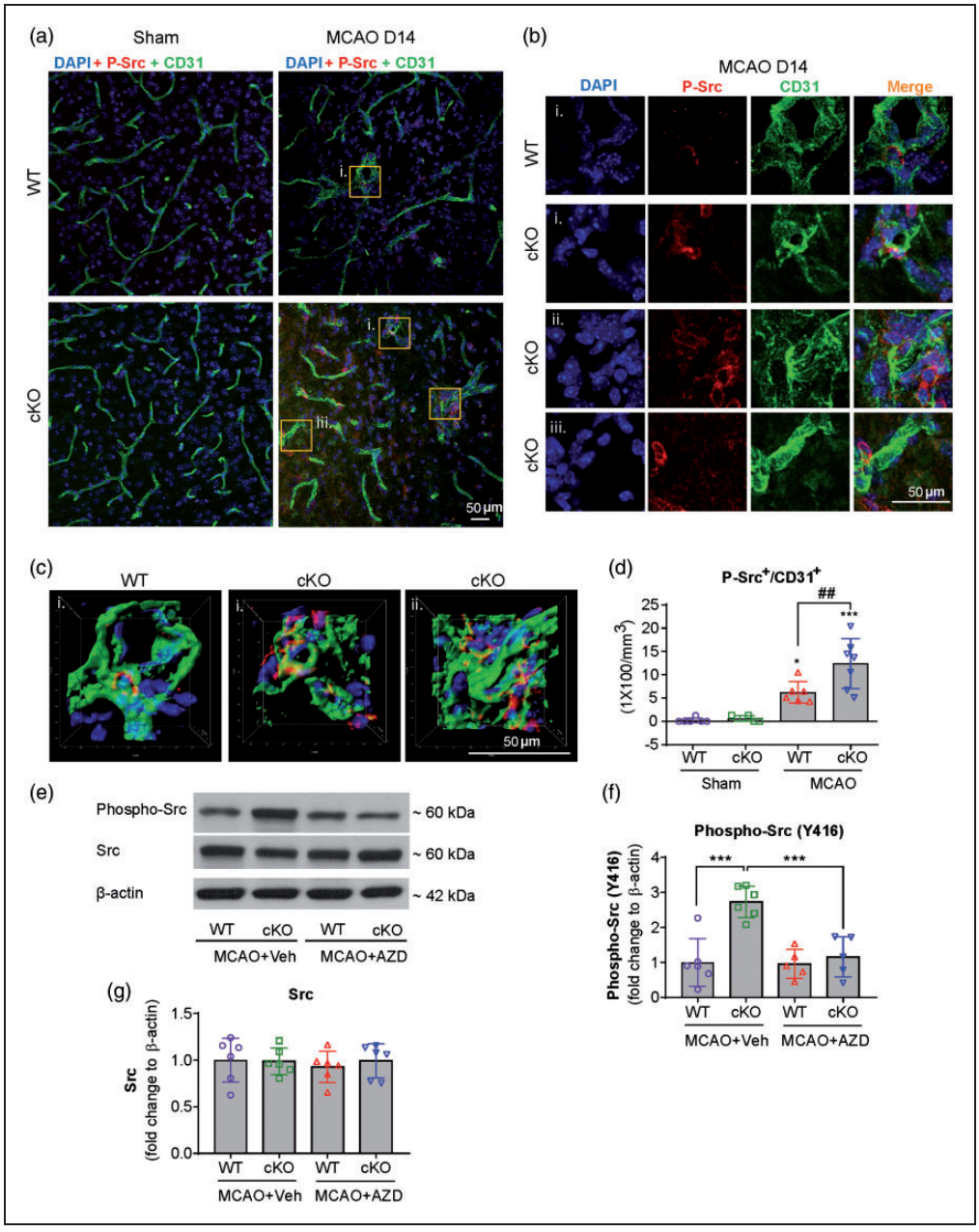

Figure 1. Src kinase is activated in the peri-infarct regions of EC-targeted miR-15a/16-1 cKO mouse brains after cerebral ischemia. EC-miR-15a/16-1 cKO mice and WT littermate controls were subjected to 1 h MCAO followed by 14d reperfusion. Vehicle (Veh) or AZD0530 (AZD, 20 mg/kg) was administered daily to both genotypes 3–14d after MCAO by oral gavage. CD31 (green), phosphorylated-Src (Y416) (red), and DAPI (blue) triple-immunostaining was utilized to determine the co-localization of cerebral microvessels and activated Src kinase in the peri-infarct regions of the ischemic brains. Yellow boxes indicated areas in (a) that were enlarged in (b) and partly 3D reconstructed in (c). DAPI, 4′,6-diamidino-2-phenylindole. (a–d) Representative images (a–c) and quantitative analysis (d) demonstrated enhanced phosphorylated-Src signals co-localized with cerebral microvessels in the peri-infarcted areas of miR-15a/16-1 cKO mice brains, compared to WT controls. There was almost no positive phosphorylated-Src signals in the sham controls. Data are expressed as the mean ± SD. n = 6–7/group for d. *$p < 0.05$, ***$p < 0.001$ between sham and MCAO groups for each genotype; ##$p < 0.01$ as indicated. Total proteins were also isolated from the ipsilateral cortex of ischemic brains after 14d reperfusion, and western blotting was carried out to detect the protein expression of phosphorylated-Src and total Src. (e,f) Representative western blotting images (e) and quantitative analysis (f) indicated endothelial-selective deletion of the miR-15a/16-1 cluster upregulated phosphorylated-Src (Y416), whereas AZD0530 effectively downregulated the phosphorylation of Src, without significantly altering the expression of total Src (g). Data are expressed as the mean ± SD. n = 5-6/group for f and g. *$p < 0.05$, **$p < 0.01$ as indicated. Statistical analysis was performed by one-way ANOVA followed by Bonferroni's multiple comparison tests.

phosphorylated Src in EC-miR-15a/16-1 cKO mice (***$p = 3.17 \times 10^{-4}$). AZD0530 did not significantly affect the levels of phosphorylated Src or total Src in WT mice, as compared to vehicle treatment.

AZD0530 treatment impairs cognitive functions and exacerbates brain atrophy in EC-targeted miR-15a/16-1 cKO mice, but not WT mice, after tMCAO

In order to determine whether the activated Src kinase contributes to long-term functional recovery in EC-miR-15a/16-1 cKO mice after ischemic stroke, we administrated AZD0530 (oral gavage, 20 mg/kg) or vehicle to EC-miR-15a/16-1 cKO mice and WT mice, respectively, 3-21 days following tMCAO. We performed the Morris water maze test[41] to evaluate spatial cognitive functions at 22-27 d after tMCAO (Figure 2 (a) to (d)). As shown in Figure 2(a) and (c), both vehicle-treated, post-stroke EC-miR-15a/16-1 cKO and WT mice performed with gradually reduced escape latency over the 5 days of testing, consistent with learning. Post-stroke EC-miR-15a/16-1 cKO mice found the hidden platform (escape latency) faster compared to post-stroke WT mice (*$p = 0.0267$, bracket), consistent with our previous findings that the EC-miR-15a/16-1 cKO improves outcomes following MCAO.[24] However, AZD0530 treatment significantly impaired the ability of post-stroke EC-miR-15a/16-1 cKO mice to find the platform compared vehicle treatment (23 d, $^{\&}p = 0.0268$; 24 d, $^{\&\&\&}p = 0.0004$; 25 d, $^{\&\&}p = 0.0053$; 26 d, $^{\&}p = 0.0324$). Notably, AZD0530 treatment also partially impaired the learning ability in WT mice at two time points (24 d, $^{\#}p = 0.0470$; and 26 d, $^{\#}p = 0.0220$) compared with vehicle treatment. To test spatial memory, the platform was removed after the final trial and the location of the mouse was tracked. EC-miR-15a/16-1 cKO mice spent significantly more time in the target quadrant (where the platform had been) compared to WT mice after tMCAO (Figure 2(b) and (c), $^{\&}p = 0.0208$). AZD0530 treatment significantly decreased the time spent in the target quadrant (memory) following stroke in EC-miR-15a/16-1 cKO mice compared with vehicle treatment (Figure 2(b) and (c), *$p = 0.0349$). It is worth noting that EC-miR-15a/16-1 cKO and WT mice were comparable in swimming speed when treated with vehicle or AZD0530 (Figure 2(d)), suggesting that the performance in the water maze was unaffected by speed for both genotypes with or without drug treatments. Taken together, these data suggest that the Src inhibitor AZD0530 impairs the enhancement of cognitive outcomes in EC-targeted miR-15a/16-1 cKO mice after cerebral ischemia.

We also explored whether AZD0530 affects the brain atrophy in EC-miR-15a/16-1 cKO mice after stroke, by measuring the loss of microtubule-associated protein 2 (MAP2) immunoreactivity in brain sections at 28 d after tMCAO. Representative MAP2 immunofluorescent images (Figure 2(e)) and quantitative analysis (Figure 2(f)) showed that endothelium-targeted deletion of the miR-15a/16-1 cluster reduced post-ischemic brain atrophy in comparison with WT mice. AZD0530 treatment markedly exacerbated the loss of brain tissue in the EC-miR-15a/16-1 cKO mice after tMCAO, compared to vehicle control. AZD0530 did not significantly increase the brain atrophy after tMCAO in WT mice compared to vehicle treated WT mice. We also observed the similar results for the brain atrophy percentage of the ipsilateral hemisphere to contralateral hemisphere (Figure S4). Thus, inhibition of Src with AZD0530 appears to completely reverse the gross tissue protective effects of the EC-miR-15a/16-1 cKO.

AZD0530 treatment impairs cerebral blood flow recovery in EC-targeted miR-15a/16-1 cKO mice after tMCAO

To investigate whether altered cognitive outcomes and brain atrophy after AZD0530 treatment are related to cerebral blood flow (CBF) over a long-term recovery period of ischemic stroke, we monitored the spatiotemporal changes of cortical CBF using laser speckle imaging. Two-dimensional laser speckle images were scanned and obtained from the EC-miR-15a/16-1 cKO and WT mice. Before AZD0530 or vehicle treatments commenced at 3 d following MCAO, no significant differences were observed in cortical CBF between EC-miR-15a/16-1 cKO and WT mice prior to MCAO, 15 min after the onset of MCAO, or 15 min after the onset of reperfusion (Figure S5), eliminating MCAO surgery as a confounding factor in measuring ischemic cortical CBF. Compared with WT mice, we found considerably improved cortical CBF recovery in EC-miR-15a/16-1 cKO mice at 14 d, 21 d, and 28 d after the onset of reperfusion (Figure 3(a) and (b)). Interestingly, AZD0530 treatment robustly worsened cortical CBF recovery in EC-miR-15a/16-1 cKO mice at long-term recovery periods (21 d and 28 d after the onset of reperfusion). This treatment did not significantly alter cortical CBF recovery levels in WT mice at any tested time points after cerebral ischemia. These data were consistent with the exacerbated post-ischemic cognitive impairments and brain atrophy in EC-miR-15a/16-1 cKO mice, but not in WT mice, after AZD0530 treatment described above.

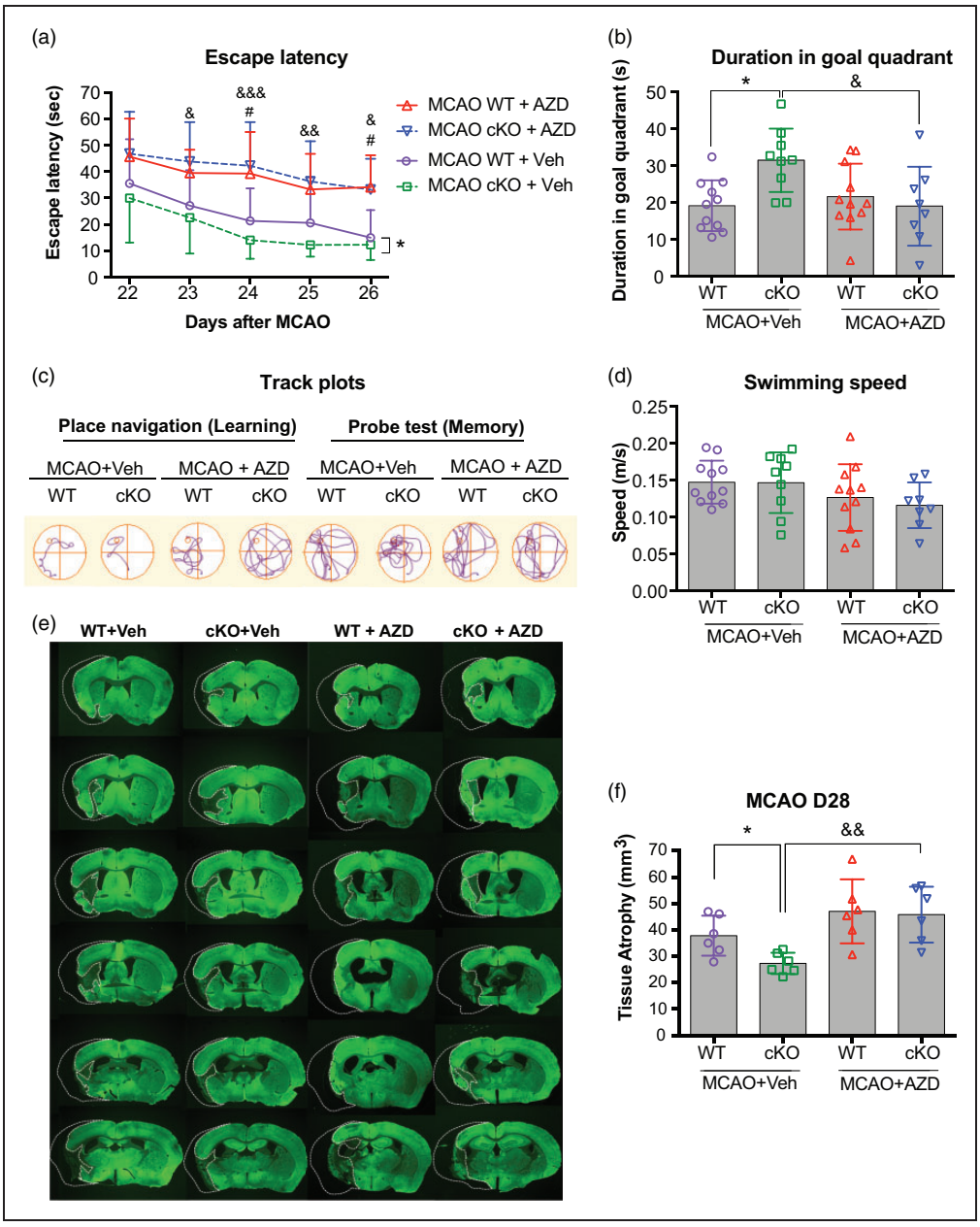

Figure 2. AZD0530 treatment impairs cognitive function and exacerbates brain atrophy in EC-targeted miR-15a/16-1 cKO mice after cerebral ischemia. EC-miR-15a/16-1 cKO mice and WT littermate controls were subjected to 1 h MCAO followed by 28d of reperfusion. Vehicle (Veh) or AZD0530 (AZD, 20 mg/kg) was administered daily to both genotypes 3-21d after MCAO by oral gavage. (a–d) Long-term cognitive functions were assessed by the Morris water maze. The time spent for the animals to locate the submerged platform (escape latency) was measured at 22-26 d after MCAO (a). Spatial memory was evaluated at 27 d after MCAO by measuring the time spent in the goal quadrant after the platform was removed (b). Representative swimming paths tracked for different experimental groups (c). Gross locomotor function was measured by average swimming speed (d), which was not affected by endothelium-targeted deletion of the miR-15a/16-1 cluster or by the treatment of AZD0530. Data are expressed as the mean ± SD. n = 11 for MCAO WT + Veh group, n = 9 for MCAO cKO + Veh group, n = 11 for MCAO WT + AZD group and n = 8 for MCAO cKO + AZD group. $^{*}p < 0.05$ between MCAO WT + Veh and MCAO cKO + Veh groups; $^{\#}p < 0.05$ between MCAO WT + Veh and MCAO WT + AZD groups; $^{\&}p < 0.05$, $^{\&\&}p < 0.01$, $^{\&\&\&}p < 0.001$ between MCAO cKO + Veh and MCAO cKO + AZD groups. (e,f) Brain atrophy was measured and quantified by microtubule-associated protein 2 (MAP2) immunostaining. Dashed lines outline the region of brain atrophy. Representative MAP2 immunofluorescent images (e), and quantitative analysis (f) showed that endothelium-targeted miR-15a/16-1 deletion reduced brain atrophy compared to WT mice, whereas AZD0530 treatment exacerbated brain atrophy in EC-miR-15a/16-1 cKO mice at 28 d after MCAO. No significant difference was found between WT + Veh and WT + AZD groups. Data are expressed as the mean ± SD. n = 6 for each group. $^{*}p < 0.05$ between MCAO WT + Veh and MCAO cKO + Veh groups; $^{\&\&}p < 0.01$ between MCAO cKO + Veh and MCAO cKO + AZD groups. Statistical analysis was performed by one-way (Figure 2(b), (d), and (f)), or two-way ANOVA (Figure 2(a)) and followed by Bonferroni's multiple comparison tests.

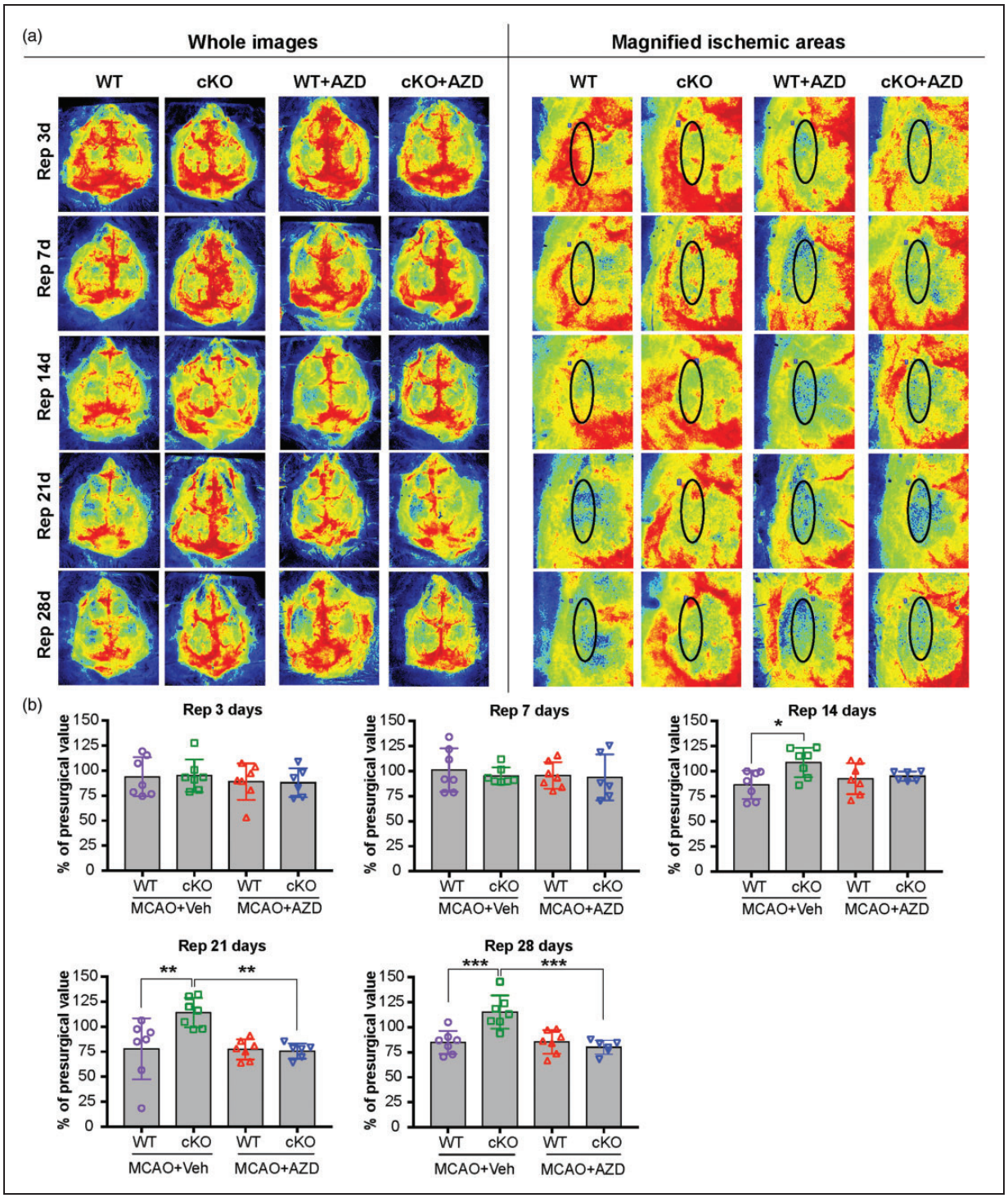

Figure 3. AZD0530 treatment attenuates CBF recovery in EC-targeted miR-15a/16-1 cKO mice at prolonged reperfusion time-points after cerebral ischemia. EC-miR-15a/16-1 cKO mice and WT littermate controls were subjected to 1 h MCAO followed by 28d reperfusion. Vehicle (Veh) or AZD0530 (AZD, 20 mg/kg) was administered daily to both genotypes at 3-21d after MCAO by oral gavage. (a–b) Representative CBF images (a) are shown at 3 d, 7 d, 14 d, 21 d and 28 d after the onset of reperfusion. Two identical elliptical ROIs were selected as indicated on the ipsilateral and contralateral hemispheres. The relative CBF was first determined as the ratio of ischemic to non-ischemic values, and then normalized to the pre-MCAO baseline for each animal. Quantitative data analysis (b) demonstrated that the relative CBF value in EC-miR-15a/16-1 cKO mice exhibited a significant increase at 14 d, 21 d and 28 d of reperfusion after MCAO under vehicle treatment. AZD0530 treatment significantly attenuated the increased CBF in EC-miR-15a/16-1 cKO mice at 21 d and 28 d reperfusion. No significant difference was found between WT + Veh and WT + AZD groups at any time point after MCAO. Data are expressed as the mean ± SD. n = 6-7 for each group. $^{*}p < 0.05$, $^{**}p < 0.01$, $^{***}p < 0.001$ as indicated. Statistical analysis was performed by one-way ANOVA followed by Bonferroni's multiple comparison tests.

AZD0530 treatment inhibits newly formed microvessels in the penumbral regions of EC-targeted miR-15a/16-1 cKO mice after tMCAO

Vascular remodeling and angiogenesis contribute to the restoration of cerebral blood flow in the ischemic cerebral hemisphere,[5,24,43] and active angiogenesis in the ischemic boundary zone (penumbra) also correlates with better survival rate in ischemic stroke patients.[5,44] To investigate whether the suppression of cortical CBF by AZD0530 treatment in EC-miR-15a/16-1 cKO mice could be attributed to inhibition of angiogenesis at long-term recovery periods after cerebral ischemia, we examined the brain microvascular structure in the peri-infarct regions 28 d after MCAO using CD31 (green) immunostaining along with BrdU (red) double-immunostaining method to identify newly formed microvessels. As shown in Figure 4(a) (upper left, bottom left), elevated CD31-positive microvascular density was observed in the ischemic brains of EC-miR-15a/16-1 cKO mice compared to WT controls. Further quantitative analysis revealed significantly higher levels of surface area ($^{\#}p = 0.0326$), vascular length ($^{\#}p = 0.0271$), and branch points ($^{\#}p = 0.0303$) in EC-miR-15a/16-1 cKO mice compared to WT controls, without AZD0530 treatment. CD31 and BrdU double-immunostaining (Figure 4(a) and (b), upper left and bottom left for each figure) and quantitative analysis (Figure 4(g) and (h)) showed that more newly formed microvessels ($BrdU^+$ cells co-labeled with $CD31^+$ microvessels) were presented EC-miR-15a/16-1 cKO mice than WT controls following tMCAO, under vehicle treatment.

Representative images (Figure 4(a) and (b), bottom right) and quantitative data illustrate that AZD0530 treatment significantly down-regulated the microvascular density in EC-miR-15a/16-1 cKO mice following MCAO in surface area (Figure 4(c), $^{***}p = 4.78 \times 10^{-7}$), vascular length (Figure 4(d), $^{***}p = 0.0003$), branch point (Figure 4(e), $^{*}p = 0.0170$), and capillary number (Figure 4(f)). Also, AZD0530 treatment markedly inhibited the generation of newly formed microvessels (Figure 4(g) and (h), $BrdU^+/CD31^+$ colocalization) in the peri-infarct regions of EC-miR-15a/16-1 cKO mice. Of note, AZD0530 treatment also robustly reduced the surface area, vascular length, and capillary number for cerebral microvasculature in ischemic WT mouse brains (Figure 4(c), (d) and (f)), but without significantly altering the amount of branch points or newly formed microvessels (Figure 4 (e) to (h)).

AZD0530 treatment inhibits the generation of new functional vessels in the peri-infarct regions of EC-targeted miR-15a/16-1 cKO mice after tMCAO

Angiogenesis involves not only the formation and growth of new, immature vessels, but also the maturation of the newly-generated vessels into perfused/functional vessels.[45] Thus, it is necessary to further investigate whether AZD0530 affects post-stroke functional angiogenesis conferred by the EC-miR-15a/16-1 cKO. As previously described,[24] biotinylated lycopersicon esculentum (tomato) lectin and BrdU double-immunostaining was utilized to determine the newly formed functional vessels. As shown in Figure S1, BrdU was injected over four consecutive days within the first week following reperfusion to identify newly formed cells, starting with the first day of AZD0530 dosing. Tomato lectin was transcardially perfused 28 d following stroke to determine whether the newly formed cells in the acute phase after stroke successfully matured into functional vessels.

As shown in Figure 5(a) (upper left vs bottom left) and Figure 5(c), (e) and (f), tomato lectin immunostaining illustrated significantly up-regulated functional vessels in EC-miR-15a/16-1 cKO mouse ischemic brains under vehicle treatment compared to WT controls, including parameters such as surface area ($^{\#}p = 0.0308$), branch points ($^{\#}p = 0.0324$), and capillary number ($^{\#}p = 0.0369$). AZD0530 treatment significantly down-regulated the density of functional vessels in EC-miR-15a/16-1 cKO mice, including surface area (Figure 5(c), $^{**}p = 0.0025$), vascular length (Figure 5 (d), $^{*}p = 0.0390$), branch points (Figure 5(e), $^{**}p = 0.0035$), and capillary number (Figure 5(f), $^{*}p = 0.0102$). In addition, BrdU/Tomato lectin double-immunostaining (Figure 5(a) and (b)) and quantitative analysis (Figure 5(g) and (h)) revealed that more newly generated cells ($BrdU^+$, $^{\#}p = 0.0276$) and more $BrdU^+$/Tomato $lectin^+$ double positive cells ($^{\#}p = 0.0238$) were present in the EC-miR-15a/16-1 cKO mice under vehicle treatment, indicating endothelium-targeted deletion of the miR-15a/16-1 cluster increased the number of newly generated functional vessels in the peri-infarct regions of ischemic brains. Representative images (Figure 5(a) and (b), bottom right) and quantitative analysis (Figure 5(g) and (h)) showed AZD0530 treatment significantly impeded the generation of newly formed functional vessels, as evidenced by fewer $BrdU^+$ positive ($^{*}p = 0.0256$) and $BrdU^+$/Tomato $lectin^+$ double positive cells ($^{**}p = 0.0087$). However, the role of

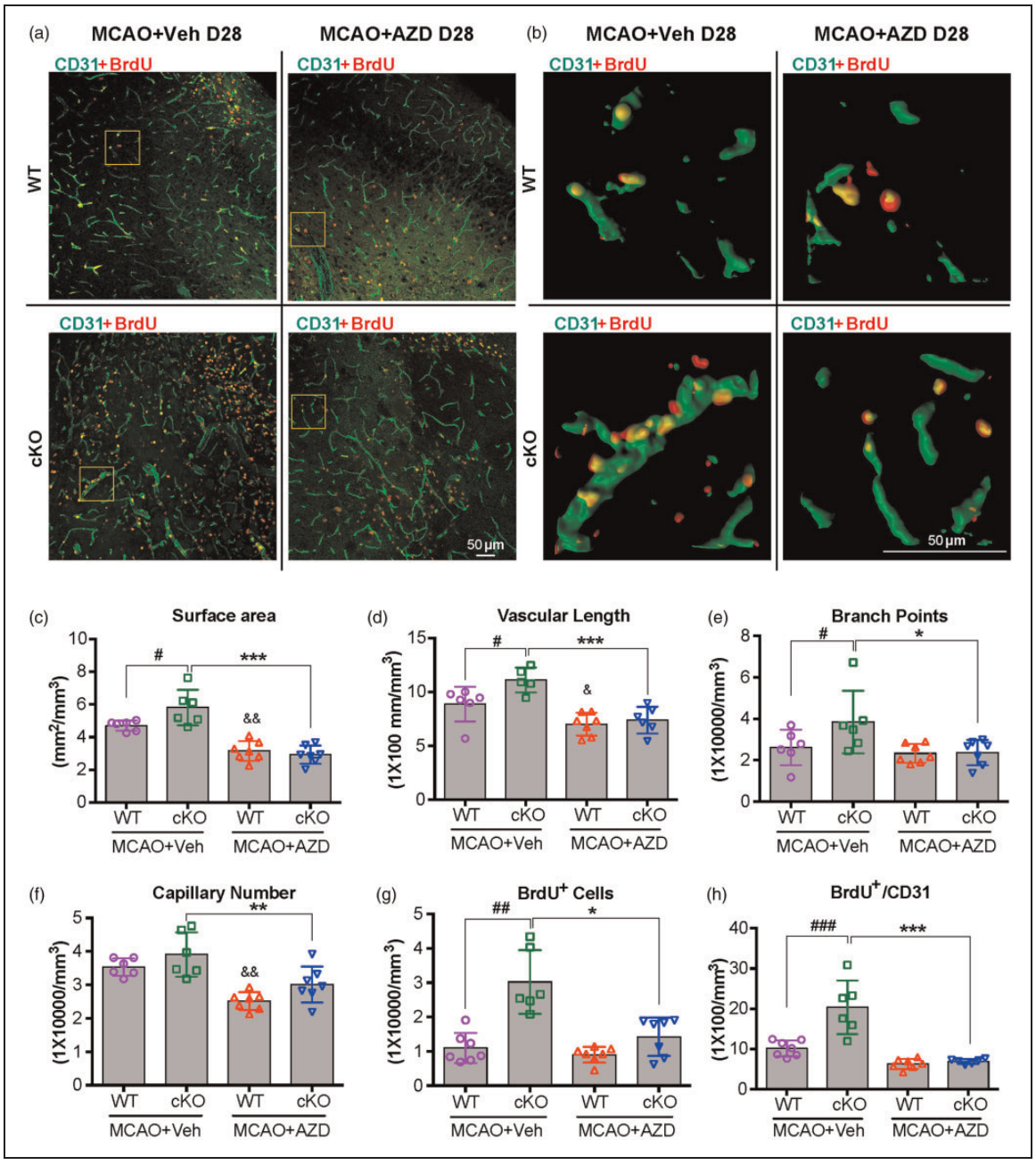

Figure 4. AZD0530 treatment inhibits the generation of newly formed microvessels in the penumbral regions of EC-targeted miR-15a/16-1 cKO mice after cerebral ischemia. EC-miR-15a/16-1 cKO mice and WT littermate controls were subjected to 1 h MCAO followed by 28d reperfusion. Vehicle (Veh) or AZD0530 (AZD, 20 mg/kg) was administered daily to both genotypes at 3-21d after MCAO by oral gavage. CD31 (green) and BrdU (red) double-immunostaining was utilized to determine the newly formed microvessels in the penumbral regions of the brains. The $BrdU^+/CD31^+$ dual-labeled signals exhibited yellow color. Yellow boxes indicated areas in (a) that were enlarged and 3D reconstructed in (b). (a–f) Representative images (a), representative 3D reconstructed images (b), quantitative analysis of surface area (c), vascular length (d), branch points (e), and capillary number (f) of CD31 immunofluorescent signal showed enhanced angiogenesis in penumbral regions of EC-miR-15a/16-1 cKO mice compared to WT controls 28 d reperfusion after MCAO, whereas AZD0530 treatment significantly downregulated the enhanced-angiogenesis in EC-miR-15a/16-1 cKO mice after cerebral ischemia. (a,b,g,h) Representative CD31 and BrdU immunofluorescent images (a), representative 3D reconstructed images (b), quantification of the $BrdU^+$ cells (g), and $BrdU^+/CD31^+$ signals (h) in the brain penumbral regions demonstrated increased newly generated cells and newly formed microvessels (angiogenesis) in the EC-miR-15a/16-1 cKO mice compared to WT controls, while AZD0530 treatment robustly inhibited angiogenesis in the EC-miR-15a/16-1 cKO mice after cerebral ischemia. Scale bar, 50 μm. Data are expressed as the mean ± SD. n = 6-7 for each group. $^{\&}p < 0.05$, $^{\&\&}p < 0.01$ between MCAO WT + Veh and MCAO WT + AZD groups; $^{*}p < 0.05$, $^{**}p < 0.01$, $^{***}p < 0.001$ between MCAO cKO +Veh and MCAO cKO + AZD groups. $^{\#}p < 0.05$, $^{\#\#}p < 0.01$, and $^{\#\#\#}p < 0.001$ as indicated. Statistical analysis was performed by one-way ANOVA followed by Bonferroni's multiple comparison tests (Figure 4(c) to (f) and (h)) or Kruskal–Wallis test followed by Dunn's multiple comparison tests (Figure 4(g)).

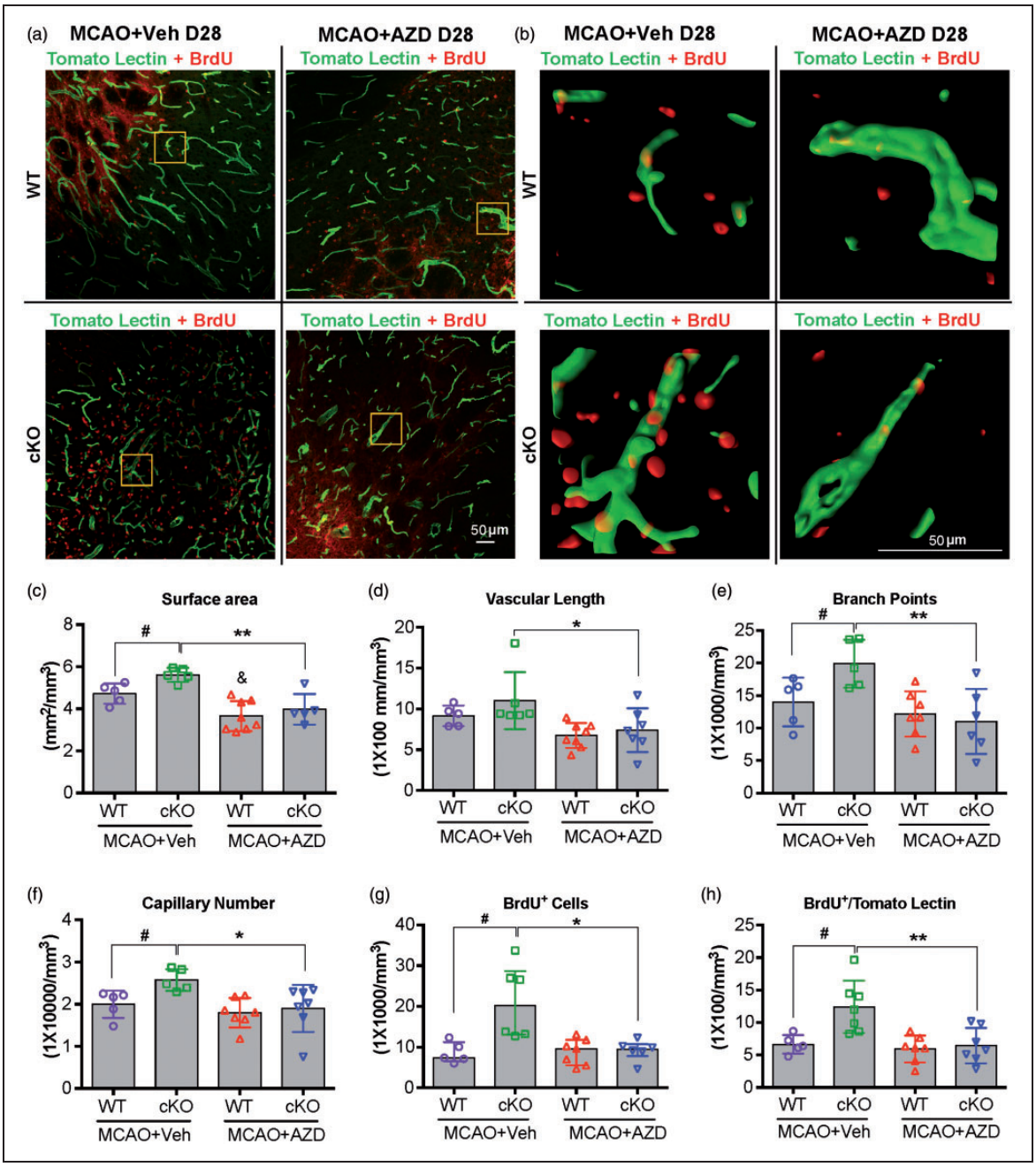

Figure 5. AZD0530 treatment impedes the generation of new functional vessels in the penumbral regions of EC-targeted miR-15a/16-1 cKO mice after cerebral ischemia. EC-miR-15a/16-1 cKO and WT littermate controls were subjected to 1 h MCAO followed by 28d reperfusion. Vehicle (Veh) or AZD0530 (AZD, 20 mg/kg) was administered daily to both genotypes at 3-21d after MCAO by oral gavage. Tomato lectin (green) and BrdU (red) double-immunofluorescent staining was utilized to detect functional microvessels in the penumbral regions. The lectin$^+$/BrdU$^+$ signals exhibit a yellow color, and the yellow boxes indicated areas in (a) were enlarged and 3 D reconstructed in (b). (a–f) Representative images (a), representative 3 D reconstructed images (b), quantitative analysis of surface area (c), vascular length (d), branch points (e), and capillary number (f) of tomato lectin immunofluorescent signal showed more functional vessels in penumbral regions of EC-miR-15a/16-1 cKO mice than WT controls at 28 d reperfusion after MCAO, whereas AZD0530 treatment reduced the upregulated-functional vessels in EC-miR-15a/16-1 cKO mice after cerebral ischemia. (a,b,g,h) Representative tomato lectin and BrdU double-immunofluorescent images (a), representative 3 D reconstructed images (b), quantification of the BrdU$^+$ cells (g) and lectin$^+$/BrdU$^+$ signals (h) in the brain penumbral regions indicate more newly generated functional vessels in the EC-miR-15a/16-1 cKO mice than WT controls, while AZD0530 treatment significantly impeded the generation of new functional vessels in the EC-miR-15a/16-1 cKO mice after cerebral ischemia. Data are expressed as the mean ± SD. n = 5-7 for each group. $^{\&}p < 0.05$ between MCAO WT + Veh and MCAO WT + AZD groups; $^{*}p < 0.05$, $^{**}p < 0.01$ between MCAO cKO + Veh and MCAO cKO + AZD groups; $^{\#}p < 0.05$ as indicated. Statistical analysis was performed by one-way ANOVA followed by Bonferroni's multiple comparison tests (Figure 5(c) to (f) and (h)) or Kruskal-Wallis test followed by Dunn's multiple comparison tests (Figure 5(g)).

AZD0530 treatment was specific in the EC-miR-15a/16-1 cKO brain after ischemia, as AZD0530 did not affect the generation of newly formed functional vessels in the peri-infarct regions of WT mice after cerebral ischemia, with the exception of surface area (Figure 5(c), $^{\&}p = 0.0189$).

Cerebral ischemia in EC-targeted miR-15a/16-1 cKO mice leads to activation of the Src signaling pathway

In order to elucidate the possible mechanism of how AZD0530 abrogates the post-stroke angiogenesis in the ischemic brains of EC-miR-15a/16-1 cKO mice, we first examined the mRNA expression levels of VEGFA, VEGFR2, FGF2 and FGFR1 in the post-stroke brain cortex by quantitative PCR (qPCR, specific primers are detailed in Table S1). Consistent with our previous findings, qPCR data (Figure S6) indicated a trend toward elevation of cortical mRNA levels of VEGFA, VEGFR2, FGF2 and FGFR1 in EC-miR-15a/16-1 cKO mice after stroke, compared to WT controls under vehicle treatment. AZD0530 treatment significantly down-regulated the cortical mRNA expression of FGF2, but not other angiogenic factors (e.g., VEGFA, VEGFR2, and FGFR1), in EC-miR-15a/16-1 cKO mice compared to vehicle treatment. As these data indicate that large changes in expression levels of growth factors do not appear to explain the potential mechanism by which AZD0530 suppresses post-stroke angiogenesis in EC-miR-15a/16-1 cKO mice, we further investigated the effects of AZD0530 on the downstream signaling mediators of these pro-angiogenic factors.

To extend our findings in Figure 1 that Src kinase is activated in peri-infarct regions of EC-miR-15a/16-1 cKO mice after stroke, we examined several key mediators directly downstream to Src kinase in mice with vehicle and AZD0530 treatment at 14 days following tMCAO by WB (specific antibodies are detailed in Table S2). Representative WB images (Figure 6(a) and (e) and Figure S10) and quantitative analysis (Figure 6(b), (c), (d), (f), and (g)) indicated that endothelium-targeted deletion of the miR-15a/16-1 cluster robustly elevated the protein expression of phosphorylated-Stat3 (Tyr-705), phosphorylated-Akt (Ser-473), phosphorylated-FAK (Tyr-397), phosphorylated-p44/42 MAPK (Thr202/Tyr204), and phosphorylated-p38 MAPK (Thr-180/Tyr182) under vehicle treatment, while AZD0530 treatment markedly abolished the protein expression of these Src signaling pathway downstream mediators. AZD0530 did not significantly influence the expression of these phosphorylated mediators in WT mice, compared to vehicle treatment. The data for total protein levels of Stat3 (Figures S7(a) and S11) and Akt (Figures S7(b) and S11) revealed no change of these factors upon genetic deletion of endothelial miR-15a/16-1, or the administration of AZD0530. Also, at 28 days following tMCAO, and we observed similar results for the Src signaling pathway related proteins under vehicle or AZD0530 treatment, except P-p44/42 MAPK, which trended toward elevation in EC-miR-15a/16-1 cKO mice under vehicle treatment (Figures S8 and S12).

Discussion

The present study demonstrates for the first time that genetic deletion of the miR-15a/16-1 cluster in endothelium promotes cerebral angiogenesis and neurological recovery through the Src signaling pathway after ischemic stroke. As illustrated in Figure 7, our data show that genetic deletion of the miR-15a/16-1 cluster in endothelium abolishes the cellular levels of miR-15a/16-1 and enhances the downstream activity of VEGF-VEGFR2 and FGF2-FGFR1 signaling cascades by triggering the phosphorylation of Src and its downstream mediators, including Akt, Stat3, p38 MAPK, and FAK. Src signaling promotes endothelial survival, proliferation, migration, and angiogenesis to boost newly generated functional vessels and regional CBF recovery, and ultimately contributes to the improved long-term neurological recovery after ischemic stroke. AZD0530, a specific pharmacological Src inhibitor, effectively blocks the phosphorylation of Src and abrogates the enhancement of VEGF-VEGFR2 and FGF2-FGFR1 signaling pathways induced by miR-15a/16-1 cKO, impeding angiogenesis and neurological recovery after cerebral ischemia. Our study thus confirmed the critical role that Src kinase plays in EC-miR-15a/16-1 genetic deletion-mediated proangiogenic effects in a mouse model of ischemic stroke.

By generating new capillaries from existing blood vessels, angiogenesis plays a critical role in organ development and tissue repair under physiological or certain pathological conditions. Increasing evidence also suggests that angiogenesis can respond to hypoxia and contribute to neovascularization in adult brains after cerebral ischemia.[46] Enhanced angiogenesis in the peri-infarct regions of ischemic stroke brain is correlated with longer post-stroke survival and better neurological outcomes.[5,24,44,47] In this context, several miRNAs have been reported to stimulate cerebral angiogenesis and improve post-stroke neurological outcomes. For example, Doeppner et al. demonstrated that virus-mediated miR-124 delivery to the striatum could enhance neurovascular remodeling such as angiogenesis and neurogenesis, probably via deubiquitinating enzyme Usp14-dependent degradation of RE1-silencing transcription factor (REST).[48] Downregulating miR-493 by its antagomir also

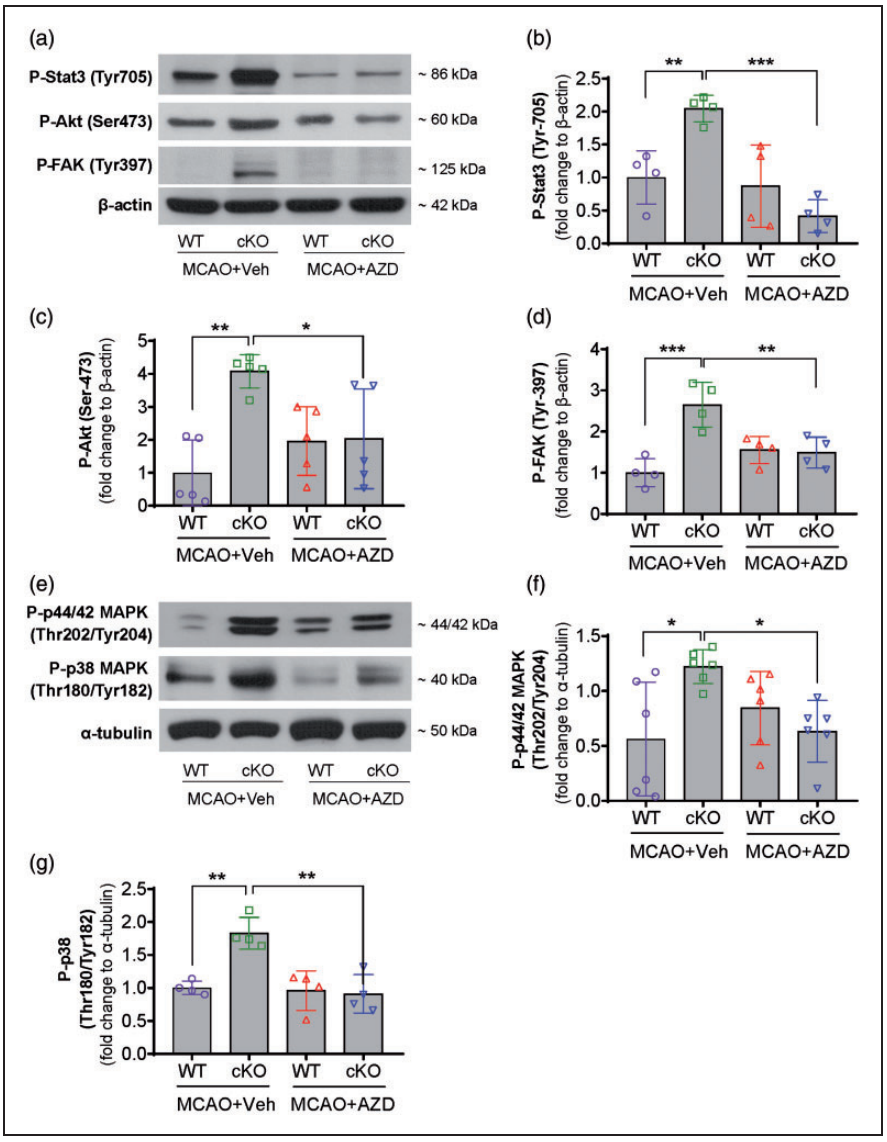

Figure 6. AZD0530 treatment blocks the Src signaling pathway in the ischemic brains of EC-targeted miR-15a/16-1 cKO mice. EC-miR-15a/16-1 cKO mice and WT littermate controls were subjected to 1 h MCAO followed by 14d reperfusion. Vehicle (Veh) or AZD0530 (AZD, 20 mg/kg) was administered daily to both genotypes at 3-14d after MCAO by oral gavage. Total proteins were isolated from the ipsilateral cortex of ischemic brains, and western blotting was carried out to detect the expression of proteins in the Src signaling pathway. (a–g) representative western blotting images (a,e) and quantitative analysis (b,c,d,f,g) indicate endothelial-selective deletion of the miR-15a/16-1 cluster upregulated the Src signaling pathway by enhancing phosphorylated-Stat3 (Tyr-705) (b), phosphorylated-Akt (Ser-473) (c), phosphorylated-FAK (Tyr-397) (d), phosphorylated-p44/42 MAPK (Thr202/Tyr204) (f), and phosphorylated-p38 MAPK (Thr180/Tyr182) (g), whereas AZD0530 effectively downregulated the phosphorylation of these Src kinase downstream mediators (b,c,d,f,g) in the ischemic brains of EC-miR-15a/16-1 cKO mice 14d after reperfusion. Data are expressed as the mean ± SD. n = 4/group for (b,d,g). n = 5/group for (c). n = 6/group for (f). *$p < 0.05$, **$p < 0.01$, ***$p < 0.001$ as indicated. Statistical analysis was performed by one-way ANOVA followed by Bonferroni's multiple comparison tests.

increased capillary density in the ischemic penumbra by directly targeting macrophage migration inhibitory factor (MIF) to improve angiogenesis.[49] Lentiviral transfer of miR-126 into mouse brain after ischemic stroke upregulated both angiogenesis and neurogenesis by directly targeting the tyrosine-protein phosphatase non-receptor type 9 (PTPN9) as well.[50] Recently, we demonstrated that endothelium-targeted deletion of the miR-15a/16-1 cluster promotes post-stroke angiogenesis and improves long-term neurological recovery by upregulating the protein expression of key proangiogenic factors VEGFA, FGF2, and their receptors VEGFR2 and FGFR1.[24] Based on this finding, we hypothesized that Src signaling might be a possible

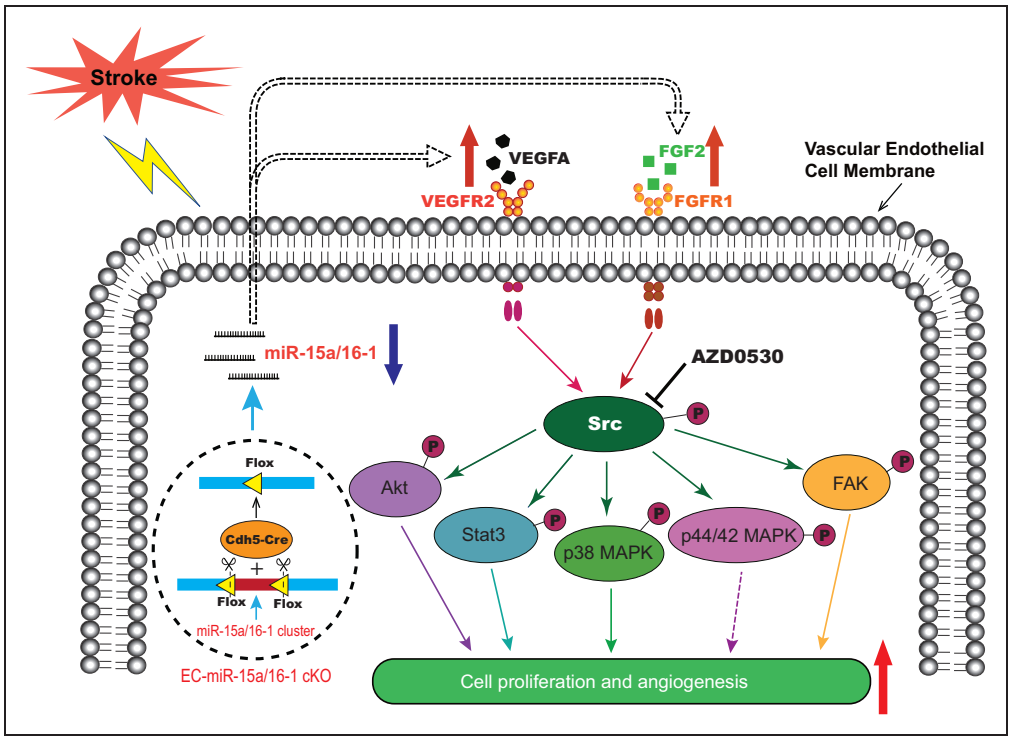

Figure 7. Graphic summary of endothelial miR-15a/16-1 in the regulation of post-stroke angiogenesis. In the stroke brain, endothelium-targeted deletion of the miR-15a/16-1 cluster (EC-miR-15a/16-1 cKO) abolishes the brain endothelial miR-15a/16-1 expression, allowing release from its translational repression of downstream key pro-angiogenic factors. This release results in the upregulation of VEGFA, FGF2 and their receptors VEGFR2 and FGFR1. The enhanced VEGF-VEGFR2, and FGF2-FGFR1 signaling cascades trigger the phosphorylation of Src and its downstream mediators, such as Akt, Stat3, p38 MAPK, p44/42 MAPK, and FAK, and promote endothelial proliferation and angiogenesis. AZD0530, a specific pharmacological inhibitor of Src, blocks the Src phosphorylation and the downstream signaling pathway, obstructing the improvement in angiogenesis in the ischemic brains of EC-miR-15a/16-1 cKO mice. VEGFA: vascular endothelial growth factor; FGF2: fibroblast growth factor 2; VEGFR2: vascular endothelial growth factor receptor 2; FGFR1: fibroblast growth factor receptor 1; Akt: protein kinase B; Stat3: signal transducer and activator of transcription 3; MAPK: mitogen-activated protein kinase; FAK: focal adhesion kinase.

downstream pathway to the above pro-angiogenic factors that could be suppressed by pharmacological Src kinase inhibitors. By using a highly selective, orally available Src kinase inhibitor AZD0530 ($IC_{50} = 2.7$ nM), we found that inhibition of Src activity efficiently negated the enhancement of cognitive outcomes, brain tissue protection, cortical CBF recovery, and formation of microvessels and functional vessels observed in EC-miR-15a/16-1 cKO mice following ischemic stroke over a long-term recovery period. Our current study not only corroborated our previous findings, but also further elucidated the downstream signaling mechanism directly underlying VEGFA and FGF2 initiated angiogenesis in cerebrovascular diseases.

Numerous growth factors triggered by an ischemic insult in the brain actively participate in the regulation of angiogenic processes following stroke. VEGFs and FGFs are well recognized as vital proangiogenic mitogens that contribute to the poststroke angiogenesis.[17,47] Prior to exploring the expression of downstream mediators of these growth factors, we investigated whether Src kinase inhibitor has any direct regulatory roles of VEGFA, VEGFR2, FGF2, and FGFR1 in the ischemic brain regions of EC-miR-15a/16-1 cKO mice. qPCR data revealed no obvious changes of VEGFA, VEGFR2 and FGFR1 mRNA expression in EC-miR-15a/16-1 cKO mouse brains following AZD0530 treatment. However, we did observe a significant reduction of mRNA levels of FGF2 in the ischemic cortex of EC-miR-15a/16-1 cKO mice. Interestingly, Nakachi et al. described that AZD0530 treatment decreased FGF2 protein levels in sensitive ovarian cancer cell lines *in vitro*, presumably through the inhibition of Src kinase phosphorylation and thereby downregulation of pituitary tumor transforming gene 1 (PTTG1).[51] In the current study, AZD0530-afforded downregulation of FGF2 in mouse brains was consistent with Nakachi's results. However, this might only be able to partially explain the compromised poststroke

angiogenesis by AZD0530, as VEGFA-VEGFR2 signaling cascade plays a dominant role in activating angiogenesis[52], but the expression of VEGFA-VEGFR2 remained unaltered after AZD0530 treatment in this study.

During the long-term recovery period following stroke, Wang et al. demonstrated that Src played a critical role in mediating angiopoietin-2-mediated cerebral angiogenesis and long-term neurovascular protection after ischemic stroke in *fat-1* transgenic mice that overproduce omega-3 polyunsaturated fatty acids.[34] Our current study focused on investigating the significance and molecular mechanism of Src kinase on endothelial miR-15a/16-1 regulated long-term post-stroke angiogenesis and neurological recovery. Consistent with Wang's findings, we found that AZD0530 blockade of Src kinase activity effectively blocked endothelial miR-15a/16-1 deletion-induced cerebral angiogenesis, including the generation of newly formed microvessels and functional vessels and CBF recovery in the ischemic cortex. Blockade of Src kinase activity by AZD0530 also hindered long-term histological and neurological recovery from cerebral ischemia afforded by the EC-miR-15a/16-1 cKO, including brain atrophy and cognitive functions in mice.

Src kinase activity is regulated by phosphorylation and dephosphorylation.[53] Our data showed increased levels of phosphorylated (Try-416) Src kinase in EC-miR-15a/16-1 cKO mice compared to WT controls following cerebral ischemia. As expected, the Src kinase inhibitor AZD0530 downregulated phosphorylated Src kinase levels in the brains of EC-miR-15a/16-1 cKO mice after stroke. We also examined the total amount of Src kinase in the isolated ischemic cortex, but no significant differences were observed between the experimental groups. We continued to investigate the Src kinase downstream signaling mediators that are associated with cell survival, proliferation, adhesion/migration, and angiogenesis.[54,55] Src kinase mediates the activation of signal transducer and activator of transcription (STAT), and inhibition of Src kinase results in dose-dependent suppression of STAT3 activity and subsequent angiogenic ability in breast cancer cells.[54,56] Src kinase is also involved in the activation of Akt to promote pro-survival signaling,[54,55] whereas inhibition of Src kinase activity can block epidermal growth factor (EGF)-induced phosphorylation/activation of Akt.[57] Moreover, Src kinase activity is essential for growth factor-induced mitogen-activated protein kinase (MAPK) activation in various cancer cell lines, which contributes to vascular endothelial cell proliferation and angiogenesis.[54,58] Furthermore, focal adhesion kinase (FAK) can be regulated by Src kinase as well,[54,55] and Src phosphorylation of FAK is a critical event that simultaneously regulates actin and adhesion dynamics and cell survival.[59] Most of these Src kinase downstream signaling cascades were reported in cancer research, some of them have been associated with post-stroke angiogenesis, including Stat3[60] and Akt.[61] In this study, we found these Src Kinase downstream regulators are involved in mediating endothelial miR-15a/16-1 deletion-enhanced poststroke brain angiogenesis through Src kinase. Our data show that the protein expression of phosphorylated-p38 MPAK (Thr-180/Tyr182), phosphorylated-p44/42 MPAK (Thr202/Tyr204), phosphorylated-Stat3 (Tyr-705), phosphorylated-Akt (Ser-473), and phosphorylated-FAK (Tyr-397) were significantly upregulated in the ischemic brain cortex of EC-miR-15a/16-1 cKO mice under vehicle treatment compared with WT ischemic brain. Inhibition of Src kinase by AZD0530 effectively eliminated these pro-angiogenic effects in EC-miR-15a/16-1 cKO mice after stroke. Thus, we suggest that activation of Src kinase and its downstream mediators p38 MAPK, p44/42 MAPK, Stat3, Akt, and FAK may synergistically contribute to endothelial miR-15a/16-1 regulated cerebral angiogenesis and neurological functions in long-term stroke recovery. Nevertheless, it is worth noting that other angiogenesis-related molecular mechanisms may be also involved, and the role of each Src kinase downstream mediator in post-stroke angiogenesis in EC-miR-15a/16-1 cKO mice may still warrant further investigation in the future.

It is also worth noting that although increased angiogenesis in the penumbral regions of ischemic brains has been evidenced to contribute to beneficial histological and functional outcomes in ischemic stroke,[17,62] newly generated capillaries may also carry pathophysiological risk effects.[63] Edema formation and hemorrhagic transformation maybe account for the most concerns due to the comprised endothelial barrier function at the early stage of brain angiogenesis/neovascularization following ischemic stroke.[63] Thus, a closely monitored investigation is required to ensure safe and effective pro-angiogenic therapeutics following ischemic stroke.[63] Interestingly, we also observed early-onset neurovascular protection, improved neurological outcomes at 3 to 7 days after ischemic stroke,[24] and ameliorated blood-brain barrier dysfunction at 1 to 2 days after ischemic stroke in EC-miR-15a/16-1 cKO mice.[64] These results suggest genetic deletion of endothelial microRNA-15a/16-1 cluster as a safe pro-angiogenic therapeutic approach for ischemic stroke.

In conclusion, the results reported here suggest that modulation of Src signaling is a critical component in the downstream signaling cascades of endothelial miR-15a/16-1-mediated regulation of post-stroke angiogenesis. Genetic deletion of endothelial miR-15a/16-1 promotes cerebral angiogenesis and

improves neurological recovery after ischemic stroke through the activation of the Src signaling pathway. With a comprehensive understanding of the molecular signaling mechanisms during cerebral neovascularization, endothelial miR-15a/16-1 may be a promising target for angiogenesis-based neurorestorative therapeutics for ischemic stroke. Moreover, our current study opens a door for miR-based vascular/endothelial therapy for ischemic stroke in the delayed reperfusion period. Elevated cerebral angiogenesis and the resulting enhancement of CBF can effectively improve the local microenvironment around salvageable penumbral brain tissues, which may facilitate neurogenesis, synaptogenesis, and oligodendrogenesis to synergistically accelerate the brain repair and improve the functional recovery after ischemic stroke. Our study also provides a theoretical basis for the combination therapy of miR-based vascular/endothelial intervention and clinical recanalization for the treatment of ischemic stroke.

Funding

The author(s) disclosed receipt of the following financial support for the research, authorship, and/or publication of this article: This work was supported by the National Institutes of Health Grant NS091175 (K.J. Yin); and American Heart Association Postdoctoral Fellowship 20POST35210900 (P. Sun); K.J. Yin is also supported by the Merit Review Grant I01BX004837 from the Department of Veterans Affairs.

Declaration of conflicting interests

The author(s) declared no potential conflicts of interest with respect to the research, authorship, and/or publication of this article.

Authors' contributions

PS and KJY designed the research; PS, FM, YX, and CZ performed the research; PS, RAS, and KJY contributed to data analysis and data interpretation; PS wrote, and RAS and KJY critically revised the paper.

Supplemental material

Supplemental material for this article is available online.

ORCID iDs

Ping Sun https://orcid.org/0000-0001-6307-3723
Feifei Ma https://orcid.org/0000-0003-1321-5564
Ke-Jie Yin https://orcid.org/0000-0002-7169-3858

References

1. Gorelick PB. The global burden of stroke: persistent and disabling. *Lancet Neurol* 2019; 18: 417–418.
2. Nozohouri S, Sifat AE, Vaidya B, et al. Novel approaches for the delivery of therapeutics in ischemic stroke. *Drug Discov Today* 2020; 25: 535–551.
3. Faralli A, Bigoni M, Mauro A, et al. Noninvasive strategies to promote functional recovery after stroke. *Neural Plast* 2013; 2013: 854597–854507.
4. Krupinski J, Kaluza J, Kumar P, et al. Some remarks on the growth-rate and angiogenesis of microvessels in ischemic stroke. Morphometric and immunocytochemical studies. *Patol Pol* 1993; 44: 203–209.
5. Krupinski J, Kaluza J, Kumar P, et al. Role of angiogenesis in patients with cerebral ischemic stroke. *Stroke* 1994; 25: 1794–1798.
6. Marti HJ, Bernaudin M, Bellail A, et al. Hypoxia-induced vascular endothelial growth factor expression precedes neovascularization after cerebral ischemia. *Am J Pathol* 2000; 156: 965–976.
7. Sun Y, Jin K, Xie L, et al. VEGF-induced neuroprotection, neurogenesis, and angiogenesis after focal cerebral ischemia. *J Clin Invest* 2003; 111: 1843–1851.
8. Chen HH, Chien CH and Liu HM. Correlation between angiogenesis and basic fibroblast growth factor expression in experimental brain infarct. *Stroke* 1994; 25: 1651–1657.
9. Issa R, AlQteishat A, Mitsios N, et al. Expression of basic fibroblast growth factor mRNA and protein in the human brain following ischaemic stroke. *Angiogenesis* 2005; 8: 53–62.
10. Iihara K, Sasahara M, Hashimoto N, et al. Induction of platelet-derived growth factor beta-receptor in focal ischemia of rat brain. *J Cereb Blood Flow Metab* 1996; 16: 941–949.
11. Iihara K, Sasahara M, Hashimoto N, et al. Ischemia induces the expression of the platelet-derived growth factor-B chain in neurons and brain macrophages in vivo. *J Cereb Blood Flow Metab* 1994; 14: 818–824.
12. Krupinski J, Kumar P, Kumar S, et al. Increased expression of TGF-beta 1 in brain tissue after ischemic stroke in humans. *Stroke* 1996; 27: 852–857.
13. Yamashita K, Gerken U, Vogel P, et al. Biphasic expression of TGF-beta1 mRNA in the rat brain following permanent occlusion of the middle cerebral artery. *Brain Res* 1999; 836: 139–145.
14. Lin TN, Wang CK, Cheung WM, et al. Induction of angiopoietin and tie receptor mRNA expression after cerebral ischemia-reperfusion. *J Cereb Blood Flow Metab* 2000; 20: 387–395.
15. Zhang Z and Chopp M. Vascular endothelial growth factor and angiopoietins in focal cerebral ischemia. *Trends Cardiovasc Med* 2002; 12: 62–66.
16. Zhang ZG, Tsang W, Zhang L, et al. Up-regulation of neuropilin-1 in neovasculature after focal cerebral ischemia in the adult rat. *J Cereb Blood Flow Metab* 2001; 21: 541–549.
17. Ergul A, Alhusban A and Fagan SC. Angiogenesis: a harmonized target for recovery after stroke. *Stroke* 2012; 43: 2270–2274.
18. Bartel DP. MicroRNAs: genomics, biogenesis, mechanism, and function. *Cell* 2004; 116: 281–297.
19. Sun P, Liu DZ, Jickling GC, et al. MicroRNA-based therapeutics in central nervous system injuries. *J Cereb Blood Flow Metab* 2018; 38: 1125–1148.

20. Yin KJ, Hamblin M and Chen YE. Angiogenesis-regulating microRNAs and ischemic stroke. *Curr Vasc Pharmacol* 2015; 13: 352–365.
21. Kuehbacher A, Urbich C and Dimmeler S. Targeting microRNA expression to regulate angiogenesis. *Trends Pharmacol Sci* 2008; 29: 12–15.
22. Calin GA, Cimmino A, Fabbri M, et al. MiR-15a and miR-16-1 cluster functions in human leukemia. *Proc Natl Acad Sci U S A* 2008; 105: 5166–5171.
23. Yang X, Tang X, Sun P, et al. MicroRNA-15a/16-1 antagomir ameliorates ischemic brain injury in experimental stroke. *Stroke* 2017; 48: 1941–1947.
24. Sun P, Zhang K, Hassan SH, et al. Endothelium-targeted deletion of microRNA-15a/16-1 promotes poststroke angiogenesis and improves long-term neurological recovery. *Circ Res* 2020; 126: 1040–1057.
25. Wu J, Du K and Lu X. Elevated expressions of serum miR-15a, miR-16, and miR-17-5p are associated with acute ischemic stroke. *Int J Clin Exp Med* 2015; 8: 21071–21079.
26. Xiang W, Tian C, Lin J, et al. Plasma let-7i and miR-15a expression are associated with the effect of recombinant tissue plasminogen activator treatment in acute ischemic stroke patients. *Thromb Res* 2017; 158: 121–125.
27. Lu WJ, Zeng LL, Wang Y, et al. Blood microRNA-15a correlates with IL-6, IGF-1 and acute cerebral ischemia. *CNR* 2018; 15: 63–71.
28. Yin KJ, Olsen K, Hamblin M, et al. Vascular endothelial cell-specific microRNA-15a inhibits angiogenesis in hindlimb ischemia. *J Biol Chem* 2012; 287: 27055–27064.
29. Schlessinger J. New roles for Src kinases in control of cell survival and angiogenesis. *Cell* 2000; 100: 293–296.
30. Eliceiri BP, Paul R, Schwartzberg PL, et al. Selective requirement for Src kinases during VEGF-induced angiogenesis and vascular permeability. *Mol Cell* 1999; 4: 915–924.
31. Sandilands E, Akbarzadeh S, Vecchione A, et al. Src kinase modulates the activation, transport and signalling dynamics of fibroblast growth factor receptors. *EMBO Rep* 2007; 8: 1162–1169.
32. Klint P, Kanda S, Kloog Y, et al. Contribution of Src and Ras pathways in FGF-2 induced endothelial cell differentiation. *Oncogene* 1999; 18: 3354–3364.
33. Paul R, Zhang ZG, Eliceiri BP, et al. Src deficiency or blockade of Src activity in mice provides cerebral protection following stroke. *Nat Med* 2001; 7: 222–227.
34. Wang J, Shi Y, Zhang L, et al. Omega-3 polyunsaturated fatty acids enhance cerebral angiogenesis and provide long-term protection after stroke. *Neurobiol Dis* 2014; 68: 91–103.
35. Percie Du Sert N, Hurst V, Ahluwalia A, et al. The ARRIVE guidelines 2.0: updated guidelines for reporting animal research. *J Cereb Blood Flow Metab* 2020; 40: 1769–1777.
36. Klein U, Lia M, Crespo M, et al. The DLEU2/miR-15a/16-1 cluster controls B cell proliferation and its deletion leads to chronic lymphocytic leukemia. *Cancer Cell* 2010; 17: 28–40.
37. Alva JA, Zovein AC, Monvoisin A, et al. VE-cadherin-Cre-recombinase transgenic mouse: a tool for lineage analysis and gene deletion in endothelial cells. *Dev Dyn* 2006; 235: 759–767.
38. Zhang X, Tang X, Liu K, et al. Long noncoding RNA Malat1 regulates cerebrovascular pathologies in ischemic stroke. *J Neurosci* 2017; 37: 1797–1806.
39. Tang X, Liu K, Hamblin MH, et al. Genetic deletion of Kruppel-like factor 11 aggravates ischemic brain injury. *Mol Neurobiol* 2018; 55: 2911–2921.
40. Shi Y, Zhang L, Pu H, et al. Rapid endothelial cytoskeletal reorganization enables early blood-brain barrier disruption and long-term ischaemic reperfusion brain injury. *Nat Commun* 2016; 7: 10523–10501.
41. Liu X, Liu J, Zhao S, et al. Interleukin-4 is essential for microglia/macrophage M2 polarization and long-term recovery after cerebral ischemia. *Stroke* 2016; 47: 498–504.
42. Jiang X, Suenaga J, Pu H, et al. Post-stroke administration of omega-3 polyunsaturated fatty acids promotes neurovascular restoration after ischemic stroke in mice: efficacy declines with aging. *Neurobiol Dis* 2019; 126: 62–75.
43. Li G, Morris-Blanco KC, Lopez MS, et al. Impact of microRNAs on ischemic stroke: from pre- to post-disease. *Prog Neurobiol* 2018; 163-164: 59–78.
44. Krupinski J, Kaluza J, Kumar P, et al. Prognostic value of blood vessel density in ischaemic stroke. *Lancet* 1993; 342: 742.
45. LeBlanc AJ, Krishnan L, Sullivan CJ, et al. Microvascular repair: post-angiogenesis vascular dynamics. *Microcirculation* 2012; 19: 676–695.
46. Greenberg DA. Poststroke angiogenesis, pro: making the desert bloom. *Stroke* 2015; 46: e101–e102.
47. Beck H and Plate KH. Angiogenesis after cerebral ischemia. *Acta Neuropathol* 2009; 117: 481–496.
48. Doeppner TR, Doehring M, Bretschneider E, et al. MicroRNA-124 protects against focal cerebral ischemia via mechanisms involving Usp14-dependent REST degradation. *Acta Neuropathol* 2013; 126: 251–265.
49. Li Q, He Q, Baral S, et al. MicroRNA-493 regulates angiogenesis in a rat model of ischemic stroke by targeting MIF. *FEBS J* 2016; 283: 1720–1733.
50. Qu M, Pan J, Wang L, et al. MicroRNA-126 regulates angiogenesis and neurogenesis in a mouse model of focal cerebral ischemia. *Mol Ther Nucleic Acids* 2019; 16: 15–25.
51. Nakachi I, Helfrich BA, Spillman MA, et al. PTTG1 levels are predictive of saracatinib sensitivity in ovarian cancer cell lines. *Clin Transl Sci* 2016; 9: 293–301.
52. Pauty J, Usuba R, Cheng IG, et al. A vascular endothelial growth factor-dependent sprouting angiogenesis assay based on an in vitro human blood vessel model for the study of anti-angiogenic drugs. *EBioMedicine* 2018; 27: 225–236.
53. Roskoski R. Jr. Src kinase regulation by phosphorylation and dephosphorylation. *Biochem Biophys Res Commun* 2005; 331: 1–14.
54. Finn RS. Targeting Src in breast cancer. *Ann Oncol* 2008; 19: 1379–1386.

55. Elsberger B. Translational evidence on the role of Src kinase and activated Src kinase in invasive breast cancer. *Crit Rev Oncol Hematol* 2014; 89: 343–351.
56. Garcia R, Bowman TL, Niu G, et al. Constitutive activation of Stat3 by the Src and JAK tyrosine kinases participates in growth regulation of human breast carcinoma cells. *Oncogene* 2001; 20: 2499–2513.
57. Kassenbrock CK, Hunter S, Garl P, et al. Inhibition of Src family kinases blocks epidermal growth factor (EGF)-induced activation of Akt, phosphorylation of c-Cbl, and ubiquitination of the EGF receptor. *J Biol Chem* 2002; 277: 24967–24975.
58. Olayioye MA, Badache A, Daly JM, et al. An essential role for Src kinase in ErbB receptor signaling through the MAPK pathway. *Exp Cell Res* 2001; 267: 81–87.
59. Westhoff MA, Serrels B, Fincham VJ, et al. SRC-mediated phosphorylation of focal adhesion kinase couples actin and adhesion dynamics to survival signaling. *Mol Cell Biol* 2004; 24: 8113–8133.
60. Hoffmann CJ, Harms U, Rex A, et al. Vascular signal transducer and activator of transcription-3 promotes angiogenesis and neuroplasticity long-term after stroke. *Circulation* 2015; 131: 1772–1782.
61. Li X, Li F, Ling L, et al. Intranasal administration of nerve growth factor promotes angiogenesis via activation of PI3K/Akt signaling following cerebral infarction in rats. *Am J Transl Res* 2018; 10: 3481–3492.
62. Kanazawa M, Takahashi T, Ishikawa M, et al. Angiogenesis in the ischemic core: a potential treatment target? *J Cereb Blood Flow Metab* 2019; 39: 753–769.
63. Rust R. Insights into the dual role of angiogenesis following stroke. *J Cereb Blood Flow Metab* 2020; 40: 1167–1171.
64. Ma F, Sun P, Zhang X, et al. Endothelium-targeted deletion of the miR-15a/16-1 cluster ameliorates blood-brain barrier dysfunction in ischemic stroke. *Sci Signal* 2020; 13: eaay5686.